

Article ID: 1000-7032(2023)03-0486-10

Perovskite Single-crystal X-ray Detectors: B-site Engineering for Future Wearable Electronics

MA Chuang, ZHAO Kui*

(Key Laboratory of Applied Surface and Colloid Chemistry, Ministry of Education, Shaanxi Key Laboratory for Advanced Energy Devices,
Shaanxi Engineering Lab for Advanced Energy Technology, Institute for Advanced Energy Materials,
School of Materials Science and Engineering, Shaanxi Normal University, Xi'an 710119, China)

* Corresponding Author, E-mail: zhaok@snnu.edu.cn

Abstract: Lead-halide perovskite single-crystal (SC) X-ray detectors have received considerable attentions due to their strong stopping power and high carrier transport efficiency. However, the application of lead-halide perovskite for wearable electronics is inhibited by their toxicity. ABX_3 hybrid perovskites have versatile structures, which enable the combination of optoelectronic properties and environmentally friendly processing through B-site engineering. In this perspective, we summarize the state of the art in perovskite SC X-ray detectors, providing an overview of B-site engineering from lead-based to lead-free and then metal-free. Later, perspective for future perovskite wearable electronics are proposed. We hope that this perspective will provide a helpful guide for structure design towards highly efficient and eco-friendly perovskite wearable electronics.

Key words: halide perovskite single-crystal; X-ray detector; B-site engineering; wearable electronics

CLC number: TL816.1; O482.31 **Document code:** A **DOI:** 10.37188/CJL.20220358

钙钛矿单晶 X 射线探测器:未来可穿戴电子器件的 B 位工程

马 闯, 赵 奎*

(陕西师范大学材料科学与工程学院, 教育部应用表面与胶体化学重点实验室, 陕西省新能源器件重点实验室,
陕西省新能源技术工程实验室, 新能源材料研究所, 陕西 西安 710119)

摘要: 卤化铅基钙钛矿单晶(SC)X射线探测器由于其强大的阻挡能力和高载流子传输效率而受到广泛关注。然而,铅基钙钛矿在可穿戴电子产品中的应用受到其毒性的限制。 ABX_3 杂化钙钛矿具有多种结构,通过B位点工程将光电子特性和环境友好处理相结合。在这篇展望中,我们总结了钙钛矿SC X射线探测器的最新进展,提供了从铅基到无铅再到无金属的B位工程概述。随后,提出了未来钙钛矿可穿戴电子器件的前景。我们希望这篇展望将为结构设计提供有益的指导,以实现高效、环保的钙钛矿可穿戴电子器件。

关键词: 卤化钙钛矿单晶; X射线探测器; B位工程; 可穿戴电子器件

1 Introduction

X-ray detection and imaging have become nec-

essary tool for non-destructive testing in the areas of medical diagnosis, security inspection, and scientific research^[1-2]. As a new generation of optoelectronic

收稿日期: 2022-09-29; 修订日期: 2022-10-26

基金项目: 国家自然科学基金(61974085); 中央高校基本科研专项资金(GK202103109, GK202201005); 陕西省科学技术厅和西北工业大学联合研究基金(2020GXLH-Z-007)

Supported by National Natural Science Foundation of China(61974085); Fundamental Research Funds for the Central Universities(GK202103109, GK202201005); Joint Research Funds of Department of Science & Technology of Shaanxi Province and Northwestern Polytechnical University(2020GXLH-Z-007)

materials, metal halide perovskites have shown great potential for application in X-ray detection due to their excellent properties, such as solution-processable, high atomic number, large attenuation coefficient, and large carrier mobility lifetime product ($\mu\tau$)^[3-4]. The general formula of metal halide perovskites is ABX_3 , where A is MA^+ (MA = methylammonium), FA^+ (FA = formamidinium) and Cs^+ ; B = metal ion; X is Cl, Br, and I. Perovskite single-crystals (SC) exhibit lower defect concentrations, smaller ion migration behavior, and better stability compared to their polycrystalline counterparts, mainly due to the absence of grain boundaries in SCs, which are ideal materials for highly sensitive X-ray detector devices^[5-7].

In terms of X-ray detection mechanism, it can be divided into direct and indirect type X-ray detection. For the indirect X-ray detectors, incident X-ray photons are converted into ultraviolet or visible light by a scintillator. The resulting radioluminescence is then detected by a photodiode and its electrical signal is recorded by an external circuit^[8]. Compared with indirect X-ray detection, direct X-ray detection can convert high-energy X-ray photons directly into photogenerated electron-hole pairs (Fig. 1(a)), which not only avoids the intermediate con-

version process of visible photons, but also helps to minimize scattering effects, thus achieving high sensitivity and spatial resolution^[9]. The relatively soft nature of halide perovskites makes it potential for the preparation of versatile and flexible wearable electronics^[10-11]. Wearable electronics is a portable device that is worn directly on the body or integrated into a person's clothing or accessories. It not only satisfies daily life by providing their diverse and intelligent functions, but also provides great convenience for monitoring physical conditions. Wearable electronics need to have large flexibility, lightweight, harmless to human body, low power consumption, high working stability. The rapid development of miniaturized applications of wearable devices has led to their extensive use in watches, bracelets, glasses, *etc.*, which in turn are interconnected with mobile terminals through wireless networks and Bluetooth technology, and eventually data analysis is performed through corresponding applications^[12-13]. Currently, halide perovskites are mostly focused on rigid X-ray detectors, while less has been reported for flexible X-ray detectors^[11,14-16]. Due to the bending property of flexible perovskite, it can be suitable for imaging in non-flat objects or narrow spaces. Meanwhile, flexible X-ray detectors can solve the compatibility

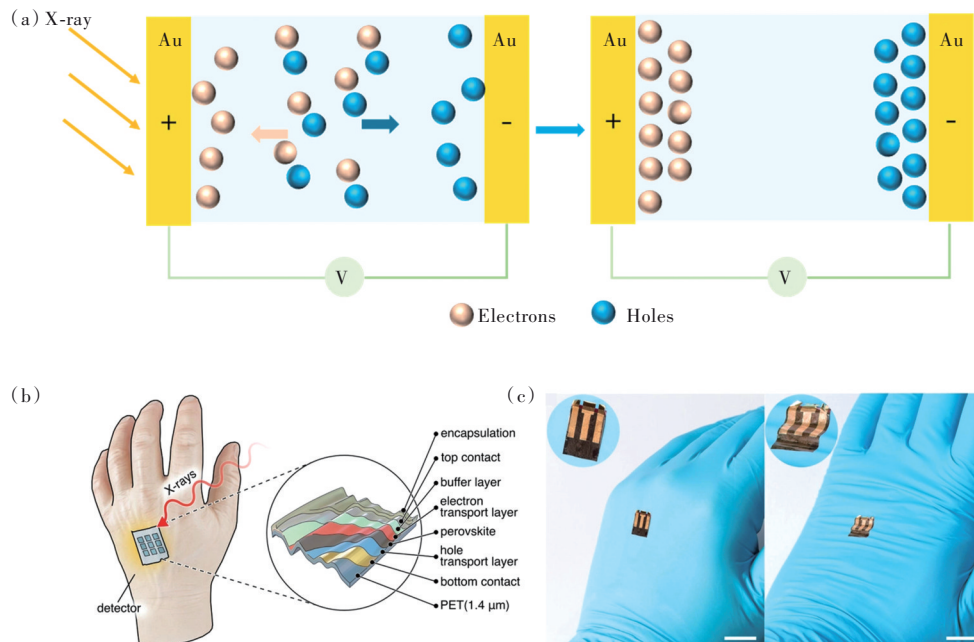


Fig. 1 (a) Schematic diagram of the working principle of direct X-ray detector. (b) Schematic diagram of flexible X-ray detector. (c) Photograph of the flexible X-ray detector on a laboratory glove^[15].

problem with non-uniform X-ray sources and reduce the misdiagnosis rate in disease screening. Kaltenbrunner *et al.* achieved the preparation of an ultra-thin flexible X-ray detector and demonstrated its application on a laboratory glove, demonstrating the advantage of adapting to complex surfaces and facilitating the development of wearable devices (Fig. 1(b)–(c))^[15]. This review provides a brief overview of the progress of direct perovskite SC X-ray detectors, then the opportunities and challenges for perovskite wearable devices are described.

2 Progress of Perovskite SC X-ray Detectors

Perovskite SCs can be divided to three types, Pb-based, Pb-free and metal-free according to ions at the *B*-site. In the following section, we present the research progress of the three types of X-ray detectors.

2.1 Pb-based Metal Halide Perovskites

In terms of Pb-based three-dimensional (3D) metal halide perovskites, it has the structural form APbX₃ (Fig. 2(a)). The presence of high atomic

number Pb makes Pb-based perovskites highly attenuate to X-rays, thus opening up their application in the field of X-ray detection. In 2013, Stoumpos *et al.* reported the first application of CsPbBr₃ SC for X-ray and γ -ray detection^[17]. In 2016, the MAPbBr₃ SC X-ray detector exhibited the sensitivity of 80 $\mu\text{C}\cdot\text{Gy}_{\text{air}}^{-1}\cdot\text{cm}^{-2}$ as reported by Huang *et al.*^[18]. Wei *et al.* achieved a sensitivity of 3 928.3 $\mu\text{C}\cdot\text{Gy}_{\text{air}}^{-1}\cdot\text{cm}^{-2}$ for the (110) facet of MAPbBr₃ SC by the facet competition management strategy (Fig. 2(b))^[19]. Subsequently, 3D MAPbI₃^[20] SC X-ray detectors were successfully applied, as well as GAMAPbI₃ (GA=guanidinium)^[21], FA_{0.55}MA_{0.45}PbI₃^[22], and FAMACs^[23] SCs obtained by component modulation, which led to a significant improvement in the detection performance of 3D Pb-based perovskites. Among them, Liu *et al.* achieved a sensitivity of $(3.5 \pm 0.2) \times 10^6 \mu\text{C}\cdot\text{Gy}_{\text{air}}^{-1}\cdot\text{cm}^{-2}$ and detection limit of 42 nGy_{air}·s⁻¹ for FAMACs SC using a triple-cation mixed halide strategy^[23]. The FAMACs SC device structures are shown in Fig. 2(c). Although Pb-based perovskite SCs based on MA⁺ and FA⁺ ions typically exhibit high sensitivity, ion migration is very pronounced

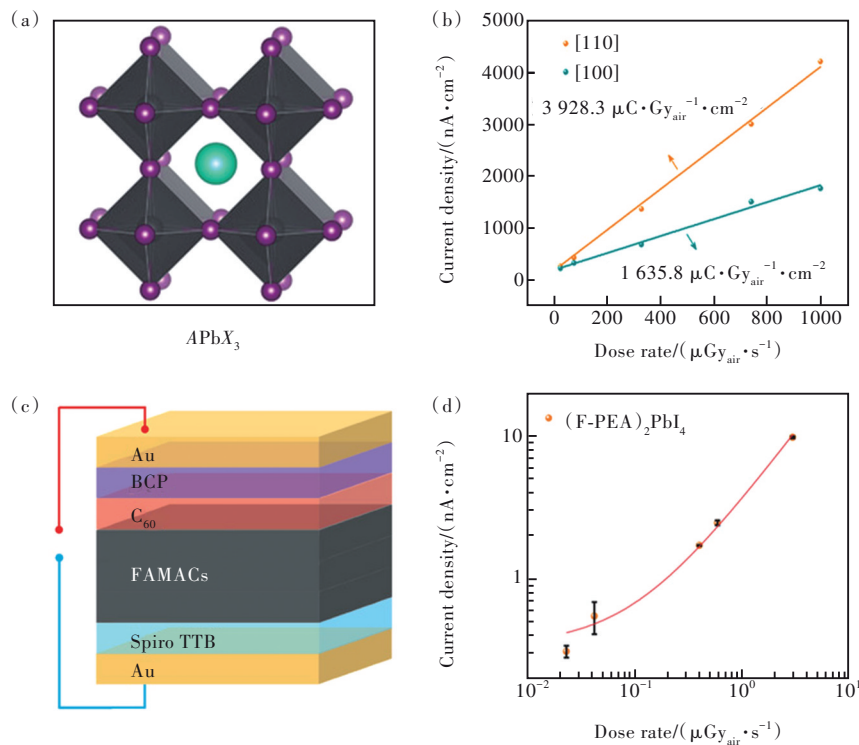


Fig. 2 (a)The crystal structure of APbX₃^[28]. (b)The plot of current density *versus* various dose rates for different facets of MAPbBr₃ SC X-ray detector^[19]. (c)The schematic diagram of FAMACs SC device structure^[23]. (d)The plot of current density *versus* various dose rates for (F-PEA)₂PbI₄ SC device^[25].

when applying a high operating electric field, causing severe dark current drift as well as being detrimental to device stability^[24]. The introduction of 2D Pb-based perovskites with large-sized organic cations increases the ion migration potential and has a significant effect on the inhibition of ion migration. Li *et al.* used (F-PEA)₂PbI₄ (F-PEA=4-fluorophenethylammonium) to enhance the supramolecular interaction between organic spacers, which in turn effectively blocked the ion migration pathway and achieved the sensitivity of $3\,402\ \mu\text{C}\cdot\text{Gy}_{\text{air}}^{-1}\cdot\text{cm}^{-2}$ as well as high operational stability (Fig. 2 (d))^[25]. Compared with 3D perovskites, low-dimensional perovskites (LDPs) exhibit significant quantum-confined effect, anisotropy, and larger band gap. Therefore, its detection performance has some gap compared with 3D perovskites^[26]. Based on the excellent air stability in LDPs, combining 3D and LDPs to fabricate high-performance, high stability X-ray detectors is an important direction for future development^[27]. Although Pb-based perovskites have large attenuation capability for X-ray and high charge extraction capability, the toxicity of elemental Pb restricts their application in wearable devices.

2.2 Pb-free Metal Halide Perovskites

Pb-based perovskite SCs contain heavy metal Pb²⁺ ions, which can cause groundwater or soil contamination if applied directly, and can accumulate in the human body after circulation and cause damage to the central nervous system and reproductive system^[29]. Therefore, B-site engineering *via* replacing Pb²⁺ by Pb-free metal ions is highly required. The preparation of Pb-free metal halide perovskites using B-site engineering can be employed by the following strategies. (1) The divalent metal M²⁺ directly replaces Pb²⁺, forming a structure similar to APbX₃ (M represents metal elements). (2) Replacement of two Pb²⁺ using a combination of monovalent M⁺ and trivalent metal ions M³⁺ constructs the called double perovskite A₂B(I)B(III)X₆ structure. (3) The molecular structure of A₂□B(IV)X₆ is obtained using tetravalent metal ions M⁴⁺ in replace of Pb²⁺. The sign of □ represents ordered vacancy. This type of crystal structure consists of a face-centered lattice with the cuboctahedral voids occupied by A-site cations, such as the reported Cs₂SnI₆ and Cs₂TeI₆^[30]. (4) The substitution of Pb²⁺ for trivalent metal ions M³⁺ can give the molecular formula of A₃□B(III)₂X₉

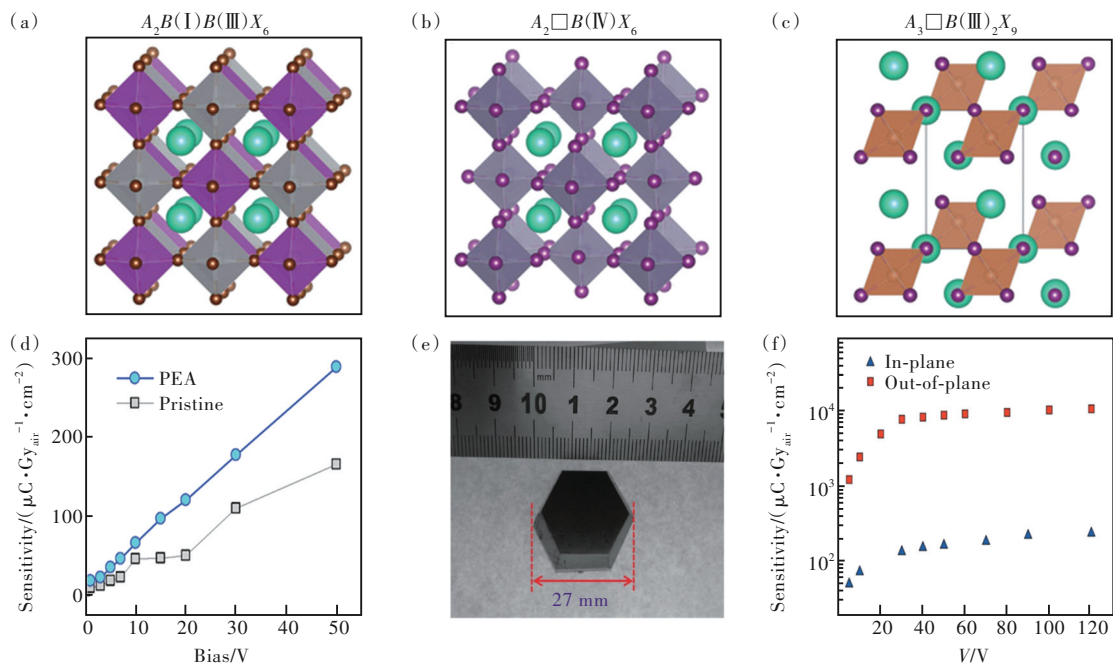


Fig. 3 The crystal structures of $A_2B(I)B(III)X_6$ (a), $A_2\Box B(IV)X_6$ (b), $A_3\Box B(III)_2X_9$ (c)^[28]. (d) The sensitivity under different bias for the pristine and PEA-Cs₂AgBiBr₆ SC device, respectively^[34]. (e) The photograph of MA₃Bi₂I₉ SC. (f) The plots of sensitivity *versus* various voltages for different MA₃Bi₂I₉ crystal planes^[37].

(Fig. 3 (a)–(c))^[28]. Among them, Bi^{3+} , which has the same electronic configuration as Pb^{2+} and a large atomic number, is a candidate material for the study of Pb-free perovskite SCs^[31]. Meanwhile, the Bi—I bond has a higher bond energy relative to the Pb—I bond, which essentially suppresses the ion migration effect and improves its structural stability^[32]. Pan *et al.* successfully prepared the first double perovskite $\text{Cs}_2\text{AgBiBr}_6$ SC X-ray detector with a sensitivity of $80 \mu\text{C}\cdot\text{Gy}_{\text{air}}^{-1}\cdot\text{cm}^{-2}$ and a low detection limit of $59.7 \text{ nGy}_{\text{air}}\cdot\text{s}^{-1}$ ^[33]. The introduction of phenylethylamine bromide (PEABr) into the $\text{Cs}_2\text{AgBiBr}_6$ precursor solution improved the ordering degree of $[\text{AgX}_6]^{5-}$ and $[\text{BiX}_6]^{3-}$ octahedra, resulting in a sensitivity of $288.8 \mu\text{C}\cdot\text{Gy}_{\text{air}}^{-1}\cdot\text{cm}^{-2}$ for the PEA- $\text{Cs}_2\text{AgBiBr}_6$ SC X-ray detector reported by Niu *et al.* (Fig. 3 (d))^[34]. Furthermore, this group optimized the crystal growth strategy to prepare higher quality $\text{Cs}_2\text{AgBiBr}_6$ SC, achieving a sensitivity of up to $1\,974 \mu\text{C}\cdot\text{Gy}_{\text{air}}^{-1}\cdot\text{cm}^{-2}$ ^[35]. In addition, Bi-based low dimensional perovskite SCs such as $(\text{NH}_4)_3\text{Bi}_2\text{I}_9$ ^[36], $\text{MA}_3\text{Bi}_2\text{I}_9$ ^[37] and $\text{FA}_3\text{Bi}_2\text{I}_9$ ^[38] have shown great promise for application. In particular, the $\text{MA}_3\text{Bi}_2\text{I}_9$ SC devices prepared by Zheng *et al.* achieved a sensitivity of $10\,620 \mu\text{C}\cdot\text{Gy}_{\text{air}}^{-1}\cdot\text{cm}^{-2}$ and a very low detection lim-

it of $0.62 \text{ nGy}_{\text{air}}\cdot\text{s}^{-1}$ ^[37], as shown in Fig. 3 (e)–(f). Pb-free metal halide perovskites have a broader variety of structural forms compared to Pb-based perovskites, which are more favorable for exploring new optoelectronic properties. However, the performance of Pb-free metal halide perovskites is highly dependent on the synthesis method, while the reproducibility of their devices remains a great challenge^[31].

2.3 Metal-free Hybrid Perovskites

Due to the presence of metal ions and the high density of these materials, it is still difficult for metal-based perovskites to be applied for wearable devices. The newly emerged metal-free perovskites, which have low toxicity, low density (lightweight), chemical tunability and promising optoelectronic properties^[39]. Metal-free hybrid perovskites have the structural formula of ABX_3 , where B is occupied by a non-metal cation, which is commonly used as NH_4^{+} ^[40] (Fig. 4 (a)). The $(\text{NH}_4)_X_6$ in the $\text{A}(\text{NH}_4)_X_3$ has larger cubic cavity relative to the PbX_6 octahedra and can accommodate large size divalent organic cation^[41]. Song *et al.* pioneered the use of DABCO- NH_4Br_3 (DABCO = *N-N'*-diazabicyclo [2.2.2] octonium) SC device to achieve a sensitivity of $173 \mu\text{C}\cdot\text{Gy}_{\text{air}}^{-1}\cdot\text{cm}^{-2}$ at $1\,250 \text{ V}\cdot\text{mm}^{-1}$ ^[42]. The photograph of

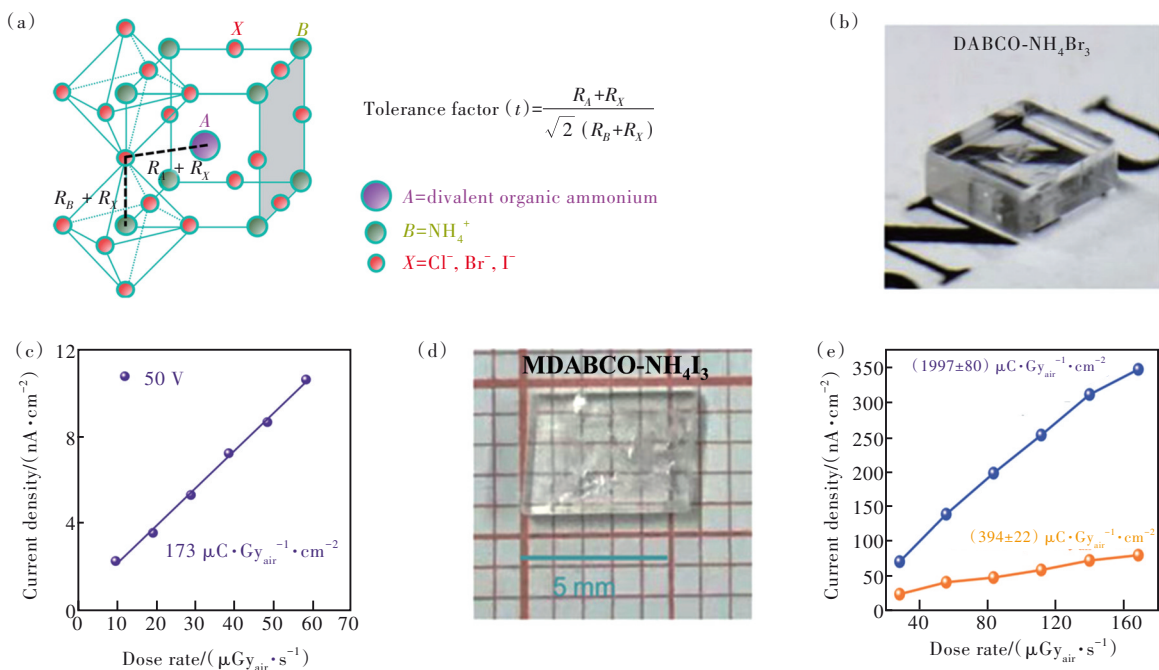


Fig. 4 (a) The crystal structure of $\text{A}(\text{NH}_4)_X_3$ ($X = \text{Cl}, \text{Br}, \text{I}$) metal-free perovskites^[41]. (b) The photograph of DABCO- NH_4Br_3 SC. (c) The plot of current density versus various dose rates for DABCO- NH_4Br_3 SC device^[42]. (d) The photograph of MDABCO- NH_4I_3 SC. (e) The plots of current density versus various dose rates for MDABCO- NH_4I_3 SC device^[43].

DABCO-NH₄Br₃ SC and the corresponding X-ray photocurrent density *versus* dose rates plots are shown in Fig. 4 (b) – (c), respectively. Based on component modulation engineering, several metal-free perovskite SCs have been exploited^[40,43-44], among which the MDABCO-NH₄I₃ (MDABCO=methyl-*N'*-diazabicyclo [2. 2. 2] octonium) SC X-ray detector achieved a sensitivity of $(1\ 997.0 \pm 80.0)\ \mu\text{C}\cdot\text{Gy}_{\text{air}}^{-1}\cdot\text{cm}^{-2[43]}$, which is the highest value in this field

so far (Fig. 4 (d) – (e)). Moreover, the MDABCO-NH₄I₃ crystal device can be completely dissolved in water, which is beneficial for the future development of biocompatible perovskite optoelectronic materials. The comparison parameters of metal-based and metal-free perovskite SC X-ray detectors are shown in Tab. 1, where the detection performance of metal-free perovskite has huge potential for development.

Tab. 1 Key parameters of the perovskite SC X-ray detectors

Kindness	Compound	X-ray energy/ keV	$\mu\tau$ product/ ($\text{cm}^2\cdot\text{V}^{-1}$)	Sensitivity/ ($\mu\text{C}\cdot\text{Gy}_{\text{air}}^{-1}\cdot\text{cm}^{-2}$)	Detection limit/ ($\text{nGy}_{\text{air}}\cdot\text{s}^{-1}$)	Ref
Pb-based	MAPbBr ₃	50	1.20×10^{-2}	80.0	500.00	[18]
	MAPbI ₃	50	—	700 000.0	1.50	[20]
	GAMAPbI ₃	40	1.25×10^{-2}	23 000.0	16.90	[21]
	FA _{0.55} MA _{0.45} PbI ₃	50	2.90×10^{-3}	87 000.0	27.70	[22]
	(F-PEA) ₂ PbI ₄	120	5.10×10^{-4}	3 402.0	23.00	[25]
	CsPbBr _{2.9} I _{0.1}	120	5.06×10^{-3}	62 748.0	117.00	[46]
	CsPbBr ₂ I		3.66×10^{-4}	492.0	54.00	
Pb-free	Cs ₂ AgBiBr ₆	30	6.30×10^{-3}	105.0	59.70	[33]
	(NH ₄) ₃ Bi ₂ I ₉	50	4.00×10^{-3}	803.0(\perp 001)	55.00	[36]
			1.10×10^{-2}	8 200.0(\parallel 001)	210.00	
	MA ₃ Bi ₂ I ₉	100	1.20×10^{-3}	10 620.0	0.62	[37]
	FA ₃ Bi ₂ I ₉	40	2.40×10^{-5}	598.1	200.00	[38]
	Cs ₃ Bi ₂ Br ₉	120	8.32×10^{-4}	1 705.0	0.58	[47-48]
		50	3.73×10^{-4}	230.4	—	
Metal-free	(DABCO)NH ₄ Br ₃	40	1.20×10^{-3}	173.0	4 960.00	[42]
	(MDABCO)NH ₄ I ₃	40	$(6.70\pm 0.33)\times 10^{-4}$	1 997.0 \pm 80.0	—	[43]
	(DABCO)NH ₄ I ₃	40	3.20×10^{-3}	567.0	—	[40]

Metal-free perovskites have the following advantages over metal-based perovskites: most of them can be prepared at room temperature in aqueous solution, which greatly reduces environmental pollution and energy consumption; the smaller density facilitates the preparation of lightweight wearable devices. Metal-free perovskites have large band gap and are not suitable for applications in the visible light. For X-ray detection, perovskite with large band gap generally produces lower noise during operation, which is beneficial for their long-term operational stability^[39]. For the preparation of flexible devices, the organic components in metal-free perovskites can soften the compound and thus facilitate the preparation of large-

area thin films. MDABCO-NH₄I₃ can be deposited on silica substrates and form uniform film without pinhole, which demonstrates the potential of metal-free perovskites for applications in wearable devices^[41,45].

3 Perspective

In summary, although the current researches on the performance of metal-based perovskite SC X-ray detectors show greater performance advantages than that of metal-free ones, the merits of metal-free halide perovskites are also incomparable. How to maximize the advantages of metal-free perovskite SCs and grow high-quality SCs for wearable devices are the focus of future research. The highlighted

perspectives are shown as follows.

(1) More attempt should be focused on designing novel metal-free perovskite SCs. At present, metal-free perovskites are mostly concentrated in 3D crystal structures, so they have a large rigidity limitation, which is not conducive to the development of flexible devices^[39]. Due to the diversity of *A*-site cations in the LDPs, the limitation of tolerance factor can be broken, and the LDPs have the more flexible crystal structures, which are easier to be applied in flexible devices. Combined with the *B*-site engineering modulation strategy, the exploration of low-dimensional metal-free perovskite SC structures can be enhanced in the future research, and then a series of effective design strategies will be developed. Meanwhile, the stability of perovskite materials has been a key factor hindering their practical applications. Although the thermal stability of metal-free perovskites has been reported, there is a lack of research on their resistance to water and oxygen in air^[3]. In the preparation of metal-free perovskites, multiple non-covalent bonding interactions between *A*-site cations and octahedras, the use of water-resistant *A*-site cations, and surface passivation strategies can be designed to enhance their stability.

(2) The researches on the optoelectronic application of metal-free halide perovskite SCs are still in its infancy stage, so systematic strategies towards surface passivation, device structure optimization have not been established. This offers the new research hotspots for the preparation of efficient and lightweight X-ray detectors.

(3) Strengthen the exploration of high quality as well as high purity metal-free perovskite SCs. The metal-free perovskite SCs can be grown in aqueous solution, which solves the problem of environmental pollution by organic solvents. The main methods used to grow metal-free perovskite SCs are temperature cooling and controlled solvent evaporation methods, such as the reported DABCO-NH₄X₃

(*X* = Cl, Br, I) and MDABCO-NH₄I₃ SCs^[40,43]. However, the SCs suitable for flexible materials have not been successfully prepared. It may be possible to prepare metal-free perovskite films by space-confined method and surface tension-controlled strategy to explore their SC flexible device properties^[49]. Therefore, when exploring growth strategies for flexible metal-free SCs, the goal is also to obtain high purity materials. The obtained high purity metal-free perovskite SCs are combined with flexible substrates to prepare flexible metal-free crystal-filled materials, which will be utilized in wearable devices^[50].

(4) More attention should be paid to the flexible wearable devices. First of all, due to the different shapes of flexible devices, research on mechanically durable and highly flexible perovskite materials needs to be enhanced. As a photoactive layer, the intrinsic high mechanical stability and resistance to bending and deformation play a key role in perovskite. The flexible substrate and electrode materials matched with perovskite need to undergo mechanical performance measurements. In addition, perovskite optoelectronic devices are mostly concentrated on small area substrates, combined with roll-to-roll, slot-die coating, and blade coating technologies to achieve the preparation of large-scale flexible devices. Therefore, in-depth research on stable perovskite ink is needed^[51]. Finally, wearable devices often need to be integrated with energy source to achieve continuous energy input for optoelectronic devices. Self-driven perovskite flexible devices can also be further developed without the need for external power supply to streamline their preparation process^[12].

Notes The authors declare no competing financial interest.

Response Letter is available for this paper at: <http://cjl.lightpublishing.cn/thesisDetails#10.37188/CJL.20220358>.

References:

- [1] PENG J L, XU Y L, YAO F, *et al.* Thick-junction perovskite X-ray detectors: processing and optoelectronic considerations

- [J]. *Nanoscale*, 2022, 14(27): 9636-9647.
- [2] 孙锡娟, 夏梦玲, 许银生, 等. 钙钛矿直接型X射线探测成像研究进展 [J]. *发光学报*, 2022, 43(7): 1014-1026.
SUN X J, XIA M L, XU Y S, *et al.* Research progress of perovskite direct X-ray imaging [J]. *Chin. J. Lumin.*, 2022, 43(7): 1014-1026. (in Chinese)
- [3] PAN Z W, WU L, JIANG J Z, *et al.* Searching for high-quality halide perovskite single crystals toward X-ray detection [J]. *J. Phys. Chem. Lett.*, 2022, 13(13): 2851-2861.
- [4] SU Y R, MA W B, YANG Y. Perovskite semiconductors for direct X-ray detection and imaging [J]. *J. Semicond.*, 2020, 41(5): 051204-1-10.
- [5] CHO Y, JUNG H R, JO W. Halide perovskite single crystals: growth, characterization, and stability for optoelectronic applications [J]. *Nanoscale*, 2022, 14(26): 9248-9277.
- [6] DONG Q F, FANG Y J, SHAO Y C, *et al.* Electron-hole diffusion lengths > 175 μm in solution-grown $\text{CH}_3\text{NH}_3\text{PbI}_3$ single crystals [J]. *Science*, 2015, 347(6225): 967-970.
- [7] LIU Y, ZHENG X P, FANG Y J, *et al.* Ligand assisted growth of perovskite single crystals with low defect density [J]. *Nat. Commun.*, 2021, 12(1): 1686-1-8.
- [8] KAKAVELAKIS G, GEDDA M, PANAGIOTOPOULOS A, *et al.* Metal halide perovskites for high-energy radiation detection [J]. *Adv. Sci.*, 2020, 7(22): 2002098-1-33.
- [9] ZHOU Y, CHEN J, BAKR O M, *et al.* Metal halide perovskites for X-ray imaging scintillators and detectors [J]. *ACS Energy Lett.*, 2021, 6(2): 739-768.
- [10] WANG J T, WANG S Z, ZHOU Y H, *et al.* Flexible perovskite light-emitting diodes: progress, challenges and perspective [J]. *Sci. China Mater.*, 2023, 66: 1-21.
- [11] ZHAO J J, ZHAO L, DENG Y H, *et al.* Perovskite-filled membranes for flexible and large-area direct-conversion X-ray detector arrays [J]. *Nat. Photonics*, 2020, 14(10): 612-617.
- [12] BAO Z N, CHEN X D. Flexible and stretchable devices [J]. *Adv. Mater.*, 2016, 28(22): 4177-4179.
- [13] CHENG Y M, WANG K, XU H, *et al.* Recent developments in sensors for wearable device applications [J]. *Anal. Bioanal. Chem.*, 2021, 413(24): 6037-6057.
- [14] CIAVATTI A, SORRENTINO R, BASIRICÒ L, *et al.* High-sensitivity flexible X-ray detectors based on printed perovskite inks [J]. *Adv. Funct. Mater.*, 2021, 31(11): 2009072-1-9.
- [15] DEMCHYSHYN S, VERDI M, BASIRICÒ L, *et al.* Designing ultraflexible perovskite X-ray detectors through interface engineering [J]. *Adv. Sci.*, 2020, 7(24): 2002586-1-11.
- [16] SUN R J, WANG Z F, WANG H Q, *et al.* Micrometer-resolution X-ray imaging enabled by a flexible perovskite screen [J]. *ACS Appl. Mater. Interfaces*, 2022, 14(32): 36801-36806.
- [17] STOUMPOS C C, MALLIAKAS C D, PETERS J A, *et al.* Crystal growth of the perovskite semiconductor CsPbBr_3 : a new material for high-energy radiation detection [J]. *Cryst. Growth. Des.*, 2013, 13(7): 2722-2727.
- [18] WEI H T, FANG Y J, MULLIGAN P, *et al.* Sensitive X-ray detectors made of methylammonium lead tribromide perovskite single crystals [J]. *Nat. Photonics*, 2016, 10(5): 333-339.
- [19] SONG J M, FENG X P, LI H Y, *et al.* Facile strategy for facet competition management to improve the performance of perovskite single-crystal X-ray detectors [J]. *J. Phys. Chem. Lett.*, 2020, 11(9): 3529-3535.
- [20] SONG Y L, LI L Q, BI W H, *et al.* Atomistic surface passivation of $\text{CH}_3\text{NH}_3\text{PbI}_3$ perovskite single crystals for highly sensitive coplanar-structure X-ray detectors [J]. *Research*, 2020, 2020: 5958243-1-10.
- [21] HUANG Y M, QIAO L, JIANG Y Z, *et al.* A-site cation engineering for highly efficient MAPbI_3 single-crystal X-ray detector [J]. *Angew. Chem. Int. Ed.*, 2019, 58(49): 17834-17842.
- [22] WU J M, WANG L X, FENG A B, *et al.* Self-powered $\text{FA}_{0.55}\text{MA}_{0.45}\text{PbI}_3$ single-crystal perovskite X-ray detectors with high sensitivity [J]. *Adv. Funct. Mater.*, 2022, 32(9): 2109149-1-10.
- [23] LIU Y C, ZHANG Y X, ZHU X J, *et al.* Triple-cation and mixed-halide perovskite single crystal for high-performance X-ray imaging [J]. *Adv. Mater.*, 2021, 33(8): 2006010-1-10.
- [24] HE Y H, PAN W T, GUO C J, *et al.* 3D/2D perovskite single crystals heterojunction for suppressed ions migration in hard X-ray detection [J]. *Adv. Funct. Mater.*, 2021, 31(49): 2104880-1-8.
- [25] LI H Y, SONG J M, PAN W T, *et al.* Sensitive and stable 2D perovskite single-crystal X-ray detectors enabled by a

- supramolecular anchor [J]. *Adv. Mater.*, 2020, 32(40): 2003790-1-9.
- [26] SHEN Y, LIU Y C, YE H C, *et al.* Centimeter-sized single crystal of two-dimensional halide perovskites incorporating straight-chain symmetric diammonium ion for X-ray detection [J]. *Angew. Chem. Int. Ed.*, 2020, 59(35): 14896-14902.
- [27] HEO S, SEO G, CHO K T, *et al.* Dimensionally engineered perovskite heterostructure for photovoltaic and optoelectronic applications [J]. *Adv. Energy Mater.*, 2019, 9(45): 1902470-1-8.
- [28] XIAO Z W, SONG Z N, YAN Y F. From lead halide perovskites to lead-free metal halide perovskites and perovskite derivatives [J]. *Adv. Mater.*, 2019, 31(47): 1803792-1-22.
- [29] WANG R, WANG J T, TAN S, *et al.* Opportunities and challenges of lead-free perovskite optoelectronic devices [J]. *Trends Chem.*, 2019, 1(4): 368-379.
- [30] MAUGHAN A E, GANOSE A M, BORDELON M M, *et al.* Defect tolerance to intolerance in the vacancy-ordered double perovskite semiconductors Cs_2SnI_6 and Cs_2TeI_6 [J]. *J. Am. Chem. Soc.*, 2016, 138(27): 8453-8464.
- [31] ZHOU X F, WANG Y S, GE C Y, *et al.* Lead-free perovskite single crystals: a brief review [J]. *Crystals*, 2021, 11(11): 1329-1-14.
- [32] LI M B, LI H Y, LI W J, *et al.* Oriented 2D perovskite wafers for anisotropic X-ray detection through a fast tableting strategy [J]. *Adv. Mater.*, 2022, 34(8): 2108020-1-9.
- [33] PAN W C, WU H D, LUO J J, *et al.* $\text{Cs}_2\text{AgBiBr}_6$ single-crystal X-ray detectors with a low detection limit [J]. *Nat. Photonics*, 2017, 11(11): 726-732.
- [34] YUAN W N, NIU G D, XIAN Y M, *et al.* *In situ* regulating the order-disorder phase transition in $\text{Cs}_2\text{AgBiBr}_6$ single crystal toward the application in an X-ray detector [J]. *Adv. Funct. Mater.*, 2019, 29(20): 1900234-1-9.
- [35] YIN L X, WU H D, PAN W C, *et al.* Controlled cooling for synthesis of $\text{Cs}_2\text{AgBiBr}_6$ single crystals and its application for X-ray detection [J]. *Adv. Opt. Mater.*, 2019, 7(19): 1900491-1-8.
- [36] ZHUANG R Z, WANG X J, MA W B, *et al.* Highly sensitive X-ray detector made of layered perovskite-like $(\text{NH}_4)_3\text{Bi}_2\text{I}_9$ single crystal with anisotropic response [J]. *Nat. Photonics*, 2019, 13(9): 602-608.
- [37] ZHENG X J, ZHAO W, WANG P, *et al.* Ultrasensitive and stable X-ray detection using zero-dimensional lead-free perovskites [J]. *J. Energy Chem.*, 2020, 49: 299-306.
- [38] LI W, XIN D Y, TIE S J, *et al.* Zero-dimensional lead-free $\text{FA}_3\text{Bi}_2\text{I}_9$ single crystals for high-performance X-ray detection [J]. *J. Phys. Chem. Lett.*, 2021, 12(7): 1778-1785.
- [39] SONG X, HODES G, ZHAO K, *et al.* Metal-free organic halide perovskite: a new class for next optoelectronic generation devices [J]. *Adv. Energy Mater.*, 2021, 11(11): 2003331-1-13.
- [40] CUI Q Y, SONG X, LIU Y C, *et al.* Halide-modulated self-assembly of metal-free perovskite single crystals for bio-friendly X-ray detection [J]. *Matter*, 2021, 4(7): 2490-2507.
- [41] CUI Q Y, LIU S F, ZHAO K. Structural and functional insights into metal-free perovskites [J]. *J. Phys. Chem. Lett.*, 2022, 13(23): 5168-5178.
- [42] SONG X, CUI Q Y, LIU Y C, *et al.* Metal-free halide perovskite single crystals with very long charge lifetimes for efficient X-ray imaging [J]. *Adv. Mater.*, 2020, 32(42): 2003353-1-8.
- [43] SONG X, LI Q, HAN J, *et al.* Highly luminescent metal-free perovskite single crystal for biocompatible X-ray detector to attain highest sensitivity [J]. *Adv. Mater.*, 2021, 33(36): 2102190-1-10.
- [44] CUI Q Y, BU N, LIU X M, *et al.* Efficient eco-friendly flexible X-ray detectors based on molecular perovskite [J]. *Nano Lett.*, 2022, 22(14): 5973-5981.
- [45] SIRBU D, TSUI H C L, ALSAIF N, *et al.* Wide-band-gap metal-free perovskite for third-order nonlinear optics [J]. *ACS Photonics*, 2021, 8(8): 2450-2458.
- [46] ZHANG P, HUA Y Q, XU Y D, *et al.* Ultrasensitive and robust 120 keV hard X-ray imaging detector based on mixed-halide perovskite $\text{CsPbBr}_{3-n}\text{I}_n$ single crystals [J]. *Adv. Mater.*, 2022, 34(12): 2106562-1-11.
- [47] LI X, ZHANG P, HUA Y Q, *et al.* Ultralow detection limit and robust hard X-ray imaging detector based on inch-sized lead-free perovskite $\text{Cs}_3\text{Bi}_2\text{Br}_9$ single crystals [J]. *ACS Appl. Mater. Interfaces*, 2022, 14(7): 9340-9351.
- [48] LI X, DU X Y, ZHANG P, *et al.* Lead-free halide perovskite $\text{Cs}_3\text{Bi}_2\text{Br}_9$ single crystals for high-performance X-ray detection [J]. *Sci. China Mater.*, 2021, 64(6): 1427-1436.

- [49] LEI Y S, CHEN Y M, XU S. Single-crystal halide perovskites: opportunities and challenges [J]. *Matter*, 2021, 4(7): 2266-2308.
- [50] LI Z Z, PENG G Q, CHEN H Y, *et al.* Metal-free PAZE-NH₄X₃·H₂O perovskite for flexible transparent X-ray detection and imaging [J]. *Angew. Chem. Int. Ed.*, 2022, 61(36): e202207198-1-9.
- [51] LONG J, HUANG Z Q, ZHANG J Q, *et al.* Flexible perovskite solar cells: device design and perspective [J]. *Flex. Print. Electron*, 2020, 5(1): 013002-1-16.



马闯(1989-),男,河南洛阳人,博士,2022年于陕西师范大学获得博士学位,主要从事低维钙钛矿单晶合成以及X射线探测器应用的研究。

E-mail: machuang@snnu.edu.cn



赵奎(1983-),男,四川南充人,博士,教授,博士生导师,2009年于中国科学院获得博士学位,主要从事能源材料,包括基于有机和钙钛矿的光伏和电子器件的研究。

E-mail: zhaok@snnu.edu.cn